# Intensity correlations of a noise-driven diode laser

**G. T. Foster, S. L. Mielke, and L. A. Orozco**

*Department of Physics and Astronomy, State University of New York, Stony Brook, New York 11794-3800*

We couple noise into the driving current of a laser diode to produce correlated light. We characterize the intensity correlations of the laser with two different techniques: two-detector photon coincidence and analysis of the photocurrent from a single detector. The light exhibits bunching with a magnitude and characteristic time set by the bandwidth and the amplitude of the noise modulating the laser driving current. A simple model based on amplitude modulation of the laser intensity agrees with the measured correlation functions. The bunched light can be used to probe systems that are sensitive to intensity correlations. © 1998 Optical Society of America [S0740-3224(98)01111-4]

*OCIS codes:* 030.5260, 030.5290, 140.2020, 270.2500.

## 1. INTRODUCTION

The correlation function of the intensity gives information about the statistics and the temporal distribution of intensity fluctuations of light. For classical light the presence of intensity fluctuations will lead to bunching of photon counts detected within the time scale of high intensity fluctuations. A classical laser operated far above threshold will have zero intensity fluctuations. In a quantum-mechanical treatment the laser intensity characterized by photon number $n$ will obey Poissonian statistics. In this case, photons are just as likely to be close together as far apart in time. The intensity correlation function can be obtained by analyzing the current fluctuations out of a photodetector, or by directly measuring two photon coincidences. As a measure of fluctuation properties of light, the intensity correlation function can distinguish between a classical stochastic field and a quantum field.

Since the early measurements of lasers and Gaussian sources by Arecchi *et al.*,[1] the intensity correlation function has been used to characterize the behavior of lasers under various operating conditions. Spurred by measurements of intensity correlations of a dye laser,[2] extensive experimental[3–5] and theoretical[6–9] studies revealed the importance of multiplicative pump noise in addition to spontaneous emission in this system. Other work applied controlled multiplicative noise to a He–Ne laser to study its effects on the intensity correlations of the light.[10] The photon statistics and the intensity correlations of a free-running diode laser have also been measured.[11] In addition, an extensive body of work exists on the inherent noise of diode lasers (for a review see Ref. 12).

A well-characterized source can probe atomic systems for a dependence on the intensity correlation function of the light. Mollow[13] established the dependence of a two-photon transition rate on the specific intensity correlation of the excitation source. The response of nonlinear processes to light with different noise spectral densities has been extensively studied by Smith and collaborators at JILA.[14–17] Ryan *et al.*[18] have measured the noise characteristics of a diode laser using a nonlinear two-photon

process. Theoretical[19,20] and experimental[21] studies have shown that the rate for a two-photon transition driven by highly correlated photons from an optical parametric oscillator changes from quadratic to linear in the intensity for low intensities. In the quantum regime, Carmichael[22] and Gardiner[23] have analyzed cascaded quantum optical systems in which correlation effects in the intensity of the light are significant, requiring a non-Markovian treatment. We have started an experimental program in cascaded cavity quantum electrodynamic (QED) systems[24] to pursue studies of these non-Markovian effects.

We produce correlated light from a diode laser by adding colored pump noise. We characterize the light with measurements of the second-order intensity correlation function. The emitted light exhibits bunching. We can precisely control the noise amplitude and bandwidth to adjust the degree of bunching and correlation time of the light. We use a simple model to explain the features of the correlation in terms of the bandwidth and the amplitude of the noise. We neglect any contribution of the intrinsic quantum noise since the external modulation is large. With the laser operated below threshold, the bunching grows very large. Experimentally, we employ two different techniques to measure the intensity correlation of the light: photon coincidences measured with two detectors, and analysis of an intensity time series from the photocurrent of a single detector. This highly correlated light could be used to probe systems sensitive to non-Markovian effects.

The paper is organized as follows. In Section 2 we briefly review the intensity-correlation function and develop models to compare with our measurements. Section 3 describes the apparatus and experimental procedures. We present our results in Section 4 and our conclusions in Section 5.

## 2. THEORY

### A. Intensity Correlation Function
The normalized correlation function of a classical stochastic process, applied to the intensity of the electromagnetic field $I(t)$, is

$$g^{(2)}(\tau) = \frac{\langle I(t)I(t + \tau)\rangle}{\langle I(t)\rangle^2}, \tag{1}$$

where the brackets denote a time average.

This provides a measure of the enhancement or the suppression of intensity fluctuations relative to an ideal laser field for which $g^{(2)}(\tau) = 1$. The correlation function measures the probability distribution that, given an intensity fluctuation at time $t$, there will be another one at time $t + \tau$. The correlation function can be directly calculated from a time series of the light intensity with Eq. (1).

The value of the correlation function at $\tau = 0$ is a measurement of the statistics of the light. This is made evident by rewriting $g^{(2)}(0)$ in terms of the variance of the intensity, $\langle(\Delta I)^2\rangle = \langle I^2\rangle - \langle I\rangle^2$:

$$g^{(2)}(0) = \frac{\langle I^2\rangle}{\langle I\rangle^2} = \frac{\langle(\Delta I)^2\rangle}{\langle I\rangle^2} + 1. \tag{2}$$

For a classical source, $g^{(2)}(0) \geqslant 1$ because $\langle(\Delta I)^2\rangle \geqslant 0$. Two other conditions on the correlation function for a classical field follow from the Schwarz inequality[25]: $g^{(2)}(0) > g^{(2)}(\tau)$ and $|g^{(2)}(0) - 1| > |g^{(2)}(\tau) - 1|$. The correlation function of a classical laser is flat, since $\langle(\Delta I)^2\rangle = 0$ and $g^{(2)}(0) = 1$. Classical bunching is exhibited when intensity fluctuations are present, as defined by $[g^{(2)}(0) > g^{(2)}(0^+) > 1]$. There are nonclassical sources that violate the Schwarz inequality, producing antibunching and sub-Poissonian statistics.[26]

The quantum theory of coherence allows treatment of the intensity correlation function in terms of photons. With $I \rightarrow \hat{I}$ (normal and time ordered), $g^{(2)}(\tau)$ is the conditional probability of detecting a photon at time $t + \tau$ given that one was detected at time $t$. When $g^{(2)}(0) = 1$, the light follows Poissonian statistics, while for $g^{(2)}(0) > 1$ the statistics are super-Poissonian. If individual photons are detected, we can measure the correlation function by sending the light into an optical correlator in which photon coincidences are detected as a function of the delay time $\tau$.

### B. Linear Model

To model the effect of modulating the laser current, we assume that the intensity of the diode laser light is proportional to the injected current. This assumption is appropriate when the laser is operating significantly above threshold or below threshold. Near threshold, this is valid locally if fluctuations in the current are small. The intensity and the current are linearly related:

$$I(t) = \alpha i(t), \tag{3}$$

where the proportionality constant $\alpha$ is the above or the below threshold responsivity (mW/mA) divided by the area of the laser beam.

The laser current $i(t)$ is composed of a constant current $i_0$ that biases the diode to a particular operating point within the region above or below threshold and noise $i_{\text{noise}}(t)$ that we add from an external source. We are neglecting other noise contributions in the current source and the laser diode, such as spontaneous emission, since the external modulation is much larger:

$$i(t) = i_0 + i_{\text{noise}}(t). \tag{4}$$

The noise term averages to zero:

$$\langle i(t)\rangle = i_0. \tag{5}$$

We focus our attention on the specific case when the current noise maps directly into the intensity correlation function. This is equivalent to saying that the laser has high quantum efficiency and current fluctuations do not change its frequency. Making use of Eqs. (3)–(5), we can write Eq. (1) in terms of the currents:

$$g^{(2)}(\tau) = 1 + \frac{\langle i_{\text{noise}}(t)i_{\text{noise}}(t + \tau)\rangle}{i_0^2}. \tag{6}$$

This expression converts the correlation function of the intensity into the correlation function of the applied noise current. The noise is an independent random process, characterized by a spectral density $F(\omega)$ over a finite bandwidth. We use the Wiener–Khintchine theorem, which states that the correlation function $G(\tau)$ is the Fourier transform of the spectral density.[26] We then obtain an expression for the intensity correlation in terms of the noise-current spectral density:

$$G(\tau) = \frac{1}{\pi}\int_0^\infty F(\omega) \times \exp(-i\omega\tau)dw$$

$$= \langle i_{\text{noise}}(t)i_{\text{noise}}(t + \tau)\rangle. \tag{7}$$

We model the noise spectral density as shown in Fig. 1, with four frequencies $(a, b, c, d)$ and a power spectral density amplitude $\lambda = i_{\text{noise}}^2/\Delta f$ that is defined as the spectral power $i_{\text{noise}}^2$ in bandwidth $\Delta f$. The five constants define a trapezoidal spectrum with high- and low-pass cutoffs. We take the Fourier transform of the spectral density to obtain an analytic form of the second-order correlation function:

$$g^{(2)}(\tau) = 1 + \frac{A}{\pi}\left[\frac{(\cos d\tau - \cos c\tau)}{(c - d)\tau^2}\right.$$

$$\left. + \frac{(\cos b\tau - \cos a\tau)}{(b - a)\tau^2}\right], \tag{8}$$

with $A = \lambda/i_0^2$. For the case of noise sent through a low-pass filter $a = b = 0$, Eq. (8) reduces to
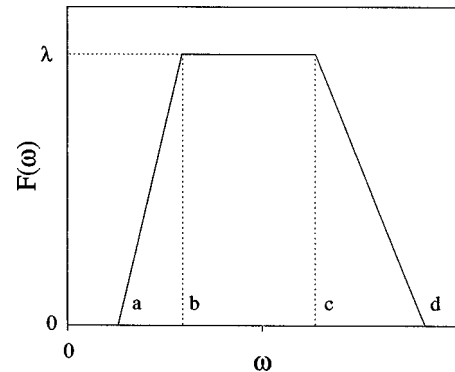


Fig. 1. Model spectral density of the noise source with five parameters $a$, $b$, $c$, $d$, and $\lambda$ to specify the spectrum and its Fourier transform.

$$g^{(2)}(\tau) = 1 + \frac{A}{\pi} \frac{(\cos d\tau - \cos c\tau)}{(c-d)\tau^2}. \qquad (9)$$

The correlation function at $\tau = 0$ is a measurement of the variance of the light intensity. For low-pass filtered noise, Eq. (9) gives

$$g^{(2)}(0) = 1 + \frac{1}{\pi} \frac{i_{\text{noise}}^2/\Delta f}{i_0^2} B, \qquad (10)$$

where $B = (c+d)/2$ is the bandwidth of the source, set by the low-pass filter cutoff frequency. Equation (10) serves as a measure of the degree of bunching of the light intensity from the diode laser.

In the limit of an infinitely sharp low-pass filter, with $a = b = 0$ and $c = d$, Eq. (9) reduces to a more familiar looking form:

$$g^{(2)}(\tau) = 1 + \frac{Ac}{\pi} \text{sinc}(c\tau). \qquad (11)$$

This simple and appealing model is valid as long as the current fluctuations remain in a linear region of the laser intensity response. Our model reproduces the result obtained analytically for a dye laser with a Fokker–Planck equation by Noriega *et al.*[9] when the correlation time of the noise is longer than the deterministic correlation time of the system. This is true despite the fact that the ratios of cavity to inversion decay times are very different in dye and diode lasers.

### C. Nonlinear Model
We take into account the nonlinear threshold response by considering a more realistic laser model. We use single-mode coupled rate equations for the photon number $n$ and excited carrier population $N$ (Ref. 27):

$$\frac{dn}{dt} = C(n+1)N - \gamma_c n, \qquad (12)$$

$$\frac{dN}{dt} = R + \sigma(t) - CnN - \gamma_{\text{rad}}N, \qquad (13)$$

where $C$ is the coupling between the excited population and the mode, $\gamma_c$ is the cavity decay rate, and $\gamma_{\text{rad}}$ is the radiative decay rate of the excited population. The pumping rate is given by $R$, and we include a pumping noise term $\sigma(t)$. The coupling coefficient is $C = \beta\gamma_{\text{rad}}$, where $\beta$ is the inverse of the cavity enhancement factor for the lasing mode.

The general approach is to map the driving current with time-dependent fluctuations into a time series of photon numbers, $n(t)$. We then calculate the normalized correlation function $g^{(2)}(\tau)$. For our calculations we use typical diode-laser parameters, $\gamma_c = 10^{12} \text{ s}^{-1}$, $\gamma_{\text{rad}} = 10^9 \text{ s}^{-1}$, and $\beta = 10^{-4}$. We numerically integrate the differential equations Eqs. (12) and (13), incrementing the noise term $\sigma(t)$ at times much shorter than the inverse of the highest-noise-frequency component. For $\sigma(t)$ we use a digitized time series of the noise sent to the laser. The highest-frequency component (10 MHz) of the noise is much lower than any of the decay rates in Eqs.

(12) and (13), so the laser intensity achieves steady state and follows the driving current over the time scale of fluctuations. This allows us to simplify numerical calculations by considering the steady-state photon number.

The steady-state solution of Eqs. (12) and (13) for the photon number in the absence of noise is

$$n_{\text{ss}} = \frac{1}{2\beta}\left[\left(\frac{R}{R_{\text{th}}} - 1\right) + \sqrt{\left(\frac{R}{R_{\text{th}}} - 1\right)^2 + 4\frac{R}{R_{\text{th}}}\beta}\right], \qquad (14)$$

with the threshold pumping rate given by $R_{\text{th}} = \gamma_c/\beta$.

We use the steady-state result Eq. (14) to calculate the intensity correlation by taking the slowly varying noisy pumping rate $R \to R + \sigma(t)$ to obtain $n_{\text{ss}}(t)$. We take the calculated photon-number time series and set it equal to a classical intensity time series. From this series we obtain the intensity correlation function using Eq. (1). The results agree quantitatively with the full numerical integration. They also reproduce the features of the simple model.

## 3. APPARATUS
We measure the correlation function using both intensity time series and photon coincidence techniques. While the first approach permits high intensities, the second requires small photon fluxes. For photon-counting measurements, one detector serves as the start for the timing of photon arrivals at a second detector. The distribution of conditional detections at this detector is proportional to the intensity correlation function. We use this detection system for other measurements investigating nonclassical features of a cavity QED system.[28] The advent of high-speed digital oscilloscopes allows photocurrents to be sampled and stored with sufficient time resolution to perform correlation measurements. The recorded time series is then used to calculate the correlation function directly. We use a single detector to measure the intensity of the laser light as a function of time. This serves as a check of our photon-counting technique.

Figure 2 shows a diagram of our apparatus. A laser current controller drives a free-running ($\sim$780-nm) diode laser (Sharp LT024) with $i_{\text{thr.}} = 59$ mA. The current driving the diode is the sum of the controller current and a capacitively coupled noise current produced by a signal generator (Stanford Research System DS 340). The DS 340 digitally generates white noise with a total bandwidth (6-dB point) of 10 MHz. We characterized the spectral density of both the voltage noise out of the DS 340 and the resulting current noise applied to the laser diode. The power spectrum of the noise applied to the la-
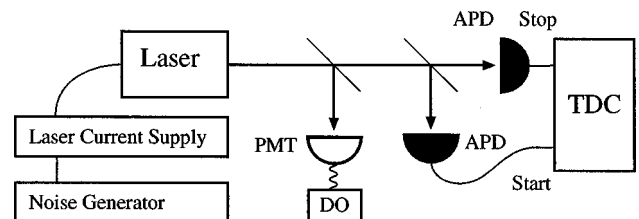


Fig. 2. Simplified diagram of the experimental setup.
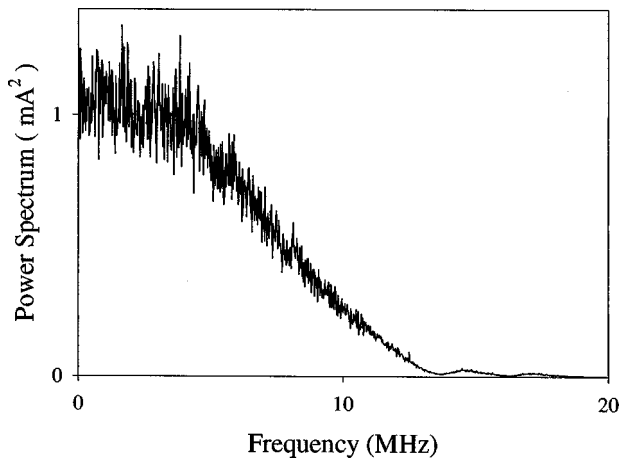
Fig. 3.   Measured power spectrum of the 10-MHz-wide noise source at the current supply output.   $\Delta f$ = 20 kHz.

ser diode is shown in Fig. 3.   We use a Lecroy 9354A digital oscilloscope (DO) to measure the power spectrum and to record a time series of the noise current for use in simulations.   Five-pole Chebyshev high- and low-pass filters shape the spectrum of the noise current and limit the bandwidth.   The modulated laser light is sent into the photon correlator.

Our photon correlator consists of two avalanche photodiodes (APD's), EG&G SPCM-AQ-151 (50% quantum efficiency), situated beyond the output ports of a 50/50 beam splitter.   Detection of a photon by APD 1 starts a Lecroy 3377 time-to-digital converter (TDC) that measures the time of detection of up to 16 consecutive photons at APD 2.   The TDC has a resolution of 0.5 ns and can measure time intervals up to 32 $\mu$s.   A delay line of 400 ns in the stop path allows coincidences at $\tau = 0$ to be observed. The location of $\tau = 0$ is determined by counting with the starts and stops provided by a 10-kHz pulser.   The directly measured delay coincides with a calculation taking into account wire lengths and electronic delays between the start and stop path.   A computer downloads and histograms the data.

To avoid the effects of detector dead time, we keep the light intensity low such that the hits/start is much less than one.   The hit/start is the number of photon counts in the stop detector during a count interval.   Coupled with the ability to register up to 16 stop events for every start, we are able to measure a close realization of $g^{(2)}(\tau)$.[29] We do not need to make a pileup correction because the rates are small enough that the event of 16 consecutive stops in a count interval is highly unlikely.   The input laser light is substantially attenuated to prevent damage to the APD's and to ensure that the number of hits per start is much less than unity.   Typical counting rates for the detectors are 100 kHz with a background count rate of less than 1 kHz.   Interference filters and polarizers in front of each detector suppress photons emitted by the APD's during the avalanche process,[30] which could lead to false counts.

We adjust the photon counters to maximize the count rates at the two detectors before taking data.   A typical count interval is 2 $\mu$s.   Data collection may take up to 10 min to achieve 100 counts per 0.5-ns bin in the long $\tau$ re-

gion.   The histogram gives directly the correlation function once we normalize it by the long-term average (between $\tau = 1.75$ and 2 $\mu$s).   For no modulation the correlation function is flat, as expected for a coherent source.   The number of hits per start for the histograms also agrees with an independently measured count rate of the number of stops.

For the single-detector technique we use a photomultiplier tube (PMT) Hamamatsu R636 to measure the light intensity.   After determining that the PMT is not saturating, the photocurrent from the PMT is sent to the digital oscilloscope that we use to store the current time series, $i(t)$, for later analysis.   We calculate $g^{(2)}(\tau)$ from the time series using Eq. (1), assuming $I(t) = i(t)$.   The comparison of the correlation measured by photon counting and from a photocurrent time series is an important check of our photon-counting technique.   Another benefit is that the operating state of the laser can be monitored in real time by observing the intensity measured by the PMT.   Mode hopping can be seen as steps in the laser intensity.   The laser can then be made single mode by a slight adjustment of the operating current.

## 4.   RESULTS

We study several different regimes to characterize the laser response to noise.   We are interested in observing a dependence on the bandwidth of the noise.   Second, we want to confirm our linear-theory dependence on the driving noise current.   Finally, we want to find a regime that maximizes the bunching.

Figure 4 shows intensity correlation function measurements for different noise bandwidths with the laser operating below threshold, $i = 56$ mA.   The bandwidth is determined by the external filters imposed on the noise source as well as by the coupling into the laser controller. The coupling cuts out the low-frequency components of the noise.   The integrated noise power coupled into the laser diode increases going from the top to the bottom of Fig. 4.   Table 1 details the measured parameters for each particular filter case.   These are determined from measurements of the noise spectrum sent to the laser diode. For low noise power the laser remains below threshold. When the bandwidth is small, the correlation function is broad and shows very little enhancement around $\tau = 0$. For larger bandwidths the presence of bunching is clear and has a sinclike character oscillating about $g^{(2)} = 1$.

Figure 5 shows plots of the linear model Eq. (8) using the measured parameters in Table 1.   The plots show qualitative agreement for all the cases.   The model plots for the two low-pass filters reproduce quantitatively the oscillations and the amplitude of the correlation measurements.   As the total noise power increases, the measured behavior differs from the linear model.

The amplitudes of the higher-bandwidth correlation functions are smaller than the model predictions.   This is due to the nonlinearity of the laser intensity near threshold.   As seen in Table 1 the integrated noise current for the direct and the 6-MHz high-pass filtered noise are larger than the low-passed noise currents.   The laser threshold region is not linear for large current excursions. In this region, negative current fluctuations decrease the
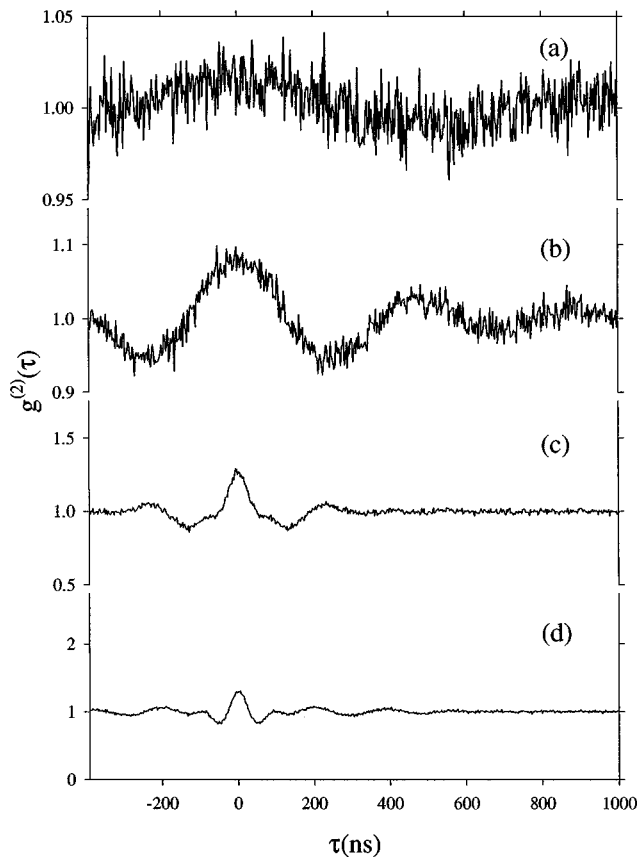
Fig. 4. Experimental plots of the correlation function for different bandwidths of the noise source and the laser operating below threshold, $i = 56$ mA:   (a) 1.2-MHz low-pass filter, (b) 2.6-MHz low-pass filter, (c) no filter, and (d) 6-MHz high-pass filter.   Note the different vertical scales.

**Table 1.   Model Parameters**

| Filter (MHz) | $a$ | $b$ | $c$ | $d$ | $\int \lambda d\omega$ (mA$^2$) |
|---|---|---|---|---|---|
| 1.2 Low pass | 0 | 1.1 | 1.1 | 1.38 | 0.88 |
| 2.6 Low pass | 0 | 2.3 | 2.3 | 2.8 | 7.2 |
| None | 0 | 4 | 8 | 14 | 43.2 |
| 6 High pass | 4 | 5.5 | 6.5 | 14 | 86.24 |

intensity less than the linear model predicts, and positive current fluctuations cause larger intensity fluctuations. This results in an increased average intensity and a decrease in the size of bunching observed.

We next investigate the intensity correlations above threshold with a laser current of $i = 64$ mA.   We apply a noise spectral density with $i_{\mathrm{noise}} \leqslant 1$ mA, including the low-frequency components.   Figure 6 shows data taken with $i_{\mathrm{noise}} = 1$ mA applied through the 2.6-MHz filter. The dashed curve shows the prediction of our linear model, Eq. (9).   The solid curve shows the calculation of the nonlinear steady-state intensity calculation.   The oscillations in the theory agree closely with the data.   The apparent background in the data from $\tau = 0$ to 500 ns may arise because of mode hops to different lasing modes, or random frequency modulation of the laser.[26]   The closer agreement of the data with the steady-state calculation demonstrates that the nonlinearity of the threshold plays an important role in the size and dynamics of the correlation function.

Figure 7 shows the dependence of $g^{(2)}(0)$ on the amplitude of the noise source for two different bandwidths (1.2 and 2.6 MHz).   The data show a quadratic dependence on the noise amplitude for low noise power.   The solid curves are plots of Eq. (10) with the measured bandwidth, operating current, and noise currents used, with no adjustable parameters.   There is good agreement for both
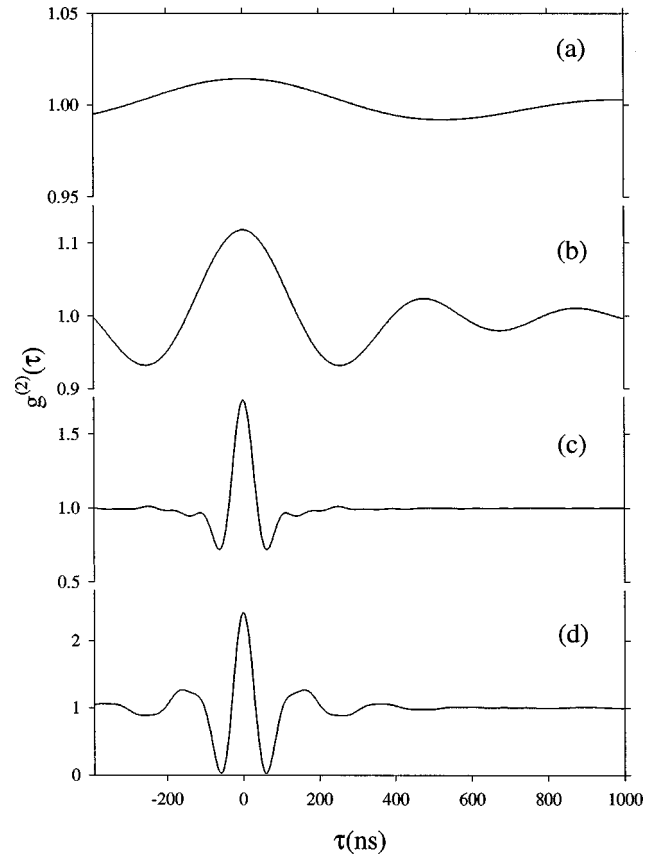


Fig. 5.   Plots of the model correlation functions [Eq. (8)] corresponding to the data of Fig. 4.   Note the different vertical scales (see Table 1 for parameters).
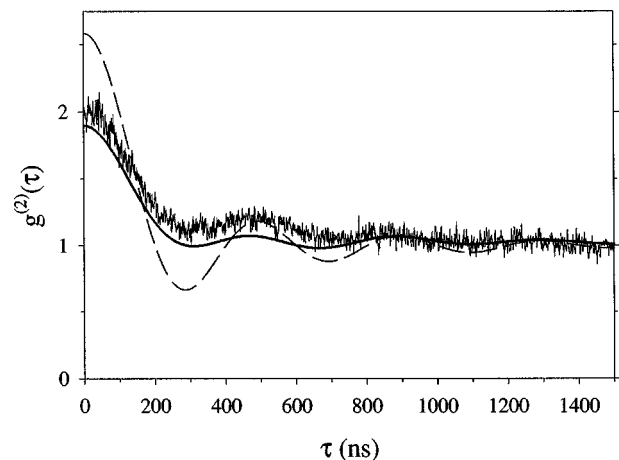


Fig. 6.   Bunching for $i_{\mathrm{noise}} = 1$ mA filtered with the 2.6-MHz low pass.   The continuous curve is a theoretical calculation based on the nonlinear model.   The dashed curve is the prediction of the linear model with $a = b = 0$, $c = 2.25$ MHz, $d = 2.75$ MHz, and $i_{\mathrm{noise}} = 1$ mA.
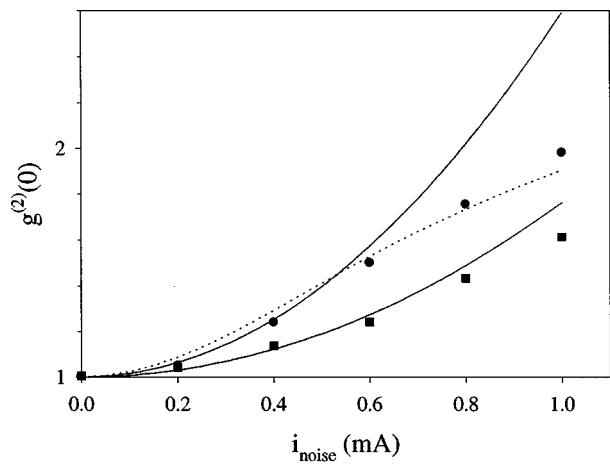
Fig. 7. Bunching as a function of applied noise current. The circles (squares) are the measured values of $g^{(2)}(0)$ for the noise modulation passing through a 2.6-MHz (1.2-MHz) low-pass filter. The solid curves are predictions based upon the linear model outlined above with no adjustable parameters. The dotted curve is a calculation with the nonlinear model ($\beta = 1.0 \times 10^{-4}$, $i_{\mathrm{thr}} = 59$ mA).
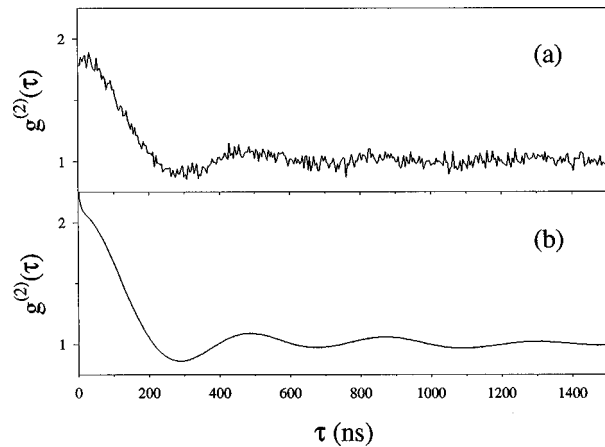


Fig. 8. Comparison of $g^{(2)}(\tau)$ from (a) photon counting and (b) from a time series of intensities measured with a single PMT.

noise bandwidths below $g^{(2)}(0) = 1.4$. The integrated noise power is the same at this point for both filters. At higher noise power the linear theory begins to separate from the measured data. When fluctuations reach threshold, the intensity no longer varies linearly with the current. This leads to an increase in the average intensity because the effect of positive current fluctuations are not balanced by negative fluctuations. Bunching decreases (since we normalize by the average intensity) as fluctuations cross threshold, as opposed to increasing, as predicted by the linear model. In Fig. 7 we see this effect above $i_{\mathrm{noise}} = 0.5$ mA for the 2.6-MHz filter. The measured values of $g^{(2)}(0)$ are less than the linear model predictions above this current.

The dotted curve is a calculation of the nonlinear model with $\beta = 1.0 \times 10^{-4}$ and $i_{\mathrm{thr}} = 0.059$ mA. This follows the data more closely than the linear model, taking into account the nonlinear threshold. We find the correlation function is very sensitive to the precise operating conditions of the laser. By adjusting the laser current down by only 0.3%, the apparent background in Fig. 6 disappears and the data points follow the model calculation better.

At this operating point we also made a comparison measurement with a single PMT as outlined above. Figure 8 shows the correlation function measured with photon counting (a) and the correlation from the PMT (b). A current of $i_{\mathrm{noise}} = 1$ mA is coupled into the laser through the 2.6-MHz filter. The PMT data are compiled from five 200-$\mu$s time series with 4-ns resolution. The photon-counting data are binned into 4-ns bins. The size and the oscillation frequency match very well for $\tau \geqslant 100$ ns. The 8-ns-wide feature at $\tau = 0$ of the PMT correlation agrees with the single-photon current pulse width. Near to $\tau = 0$, the PMT time series result exceeds the photon-counting result by 15%. This may be due to a suppression of counts owing to the 30-ns dead time of the APD.

Coupling large noise power into the laser operated below threshold leads to a significant increase in the observed bunching. Fig. 9(a) shows a measurement of the correlation function when the modulated laser is well below threshold, $i = 37$ mA. In this case the noise is sent through the 2.6-MHz low-pass filter. The results show a very large enhancement of the super-Poissonian nature of the light with large bunching evident. The light is emitted in pairs or bunches of photons that escape the laser and go into the correlator. The presence of the threshold leads to the large amplification of the correlation between photons. When the current fluctuates above threshold,
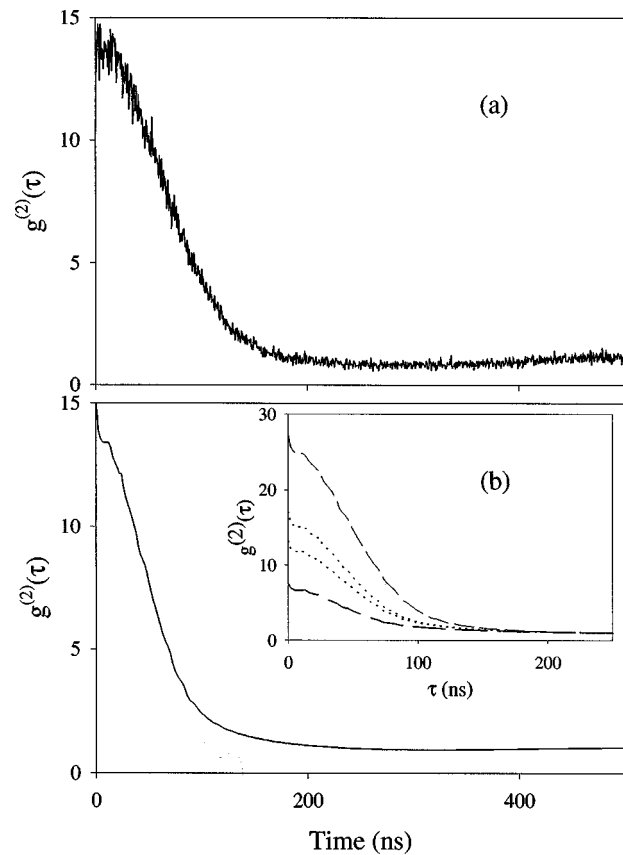


Fig. 9. Intensity correlation for noise modulation below threshold: (a) experiment and (b) simulation with $i_0 = 37.3$ mA, $i_{\mathrm{thr}} = 59$ mA, and $\beta = 0.91 \times 10^{-4}$. The inset shows the sensitivity of the peak to changes in $i_{\mathrm{thr}}$ and $\beta$. The dashed curves are the curves with $i_{\mathrm{thr}} \pm 2\%$. The dotted curves show the effect of varying $\beta$ by $\pm 10\%$.

the laser intensity increases dramatically in comparison to the average below threshold intensity.

Figure 9(b) shows $g^{(2)}(\tau)$ calculated from a time series of intensity fluctuations as outlined above. The large bunching is reproduced with the experimental parameters of the measurement. The calculated peak is narrower than the measured peak. It is possible to adjust the parameters to obtain closer agreement of the model and the measured peak, but this leads to a difference between the model and measured shape of the laser power curve.

We studied the sensitivity of the steady-state intensity model to variations in the input parameters $i_{thr}$ and $\beta$ at the operating current $i_0$. We estimate $i_{thr}$ from measurements of the laser intensity response with an uncertainty of 2%. $\beta$ is estimated to be of the order of $10^{-4}$, which produces laser response curves that are similar to the measured response. The inset of Fig. 9(b) shows how the bunching peak changes as we vary these parameters. The dashed curves show how an increase (decrease) in $i_{thr}$ by 2% leads to a substantial decrease (increase) in the peak height. Varying $\beta$ downward (upward) by 10% results in an increase (decrease) in the peak size given by the dotted lines. Above threshold at $i_0 = 64$ mA, the model is much less sensitive to changes in $i_{thr}$ and $\beta$. Increasing or decreasing $i_{thr}$ by 2% leads to a corresponding 7% increase or decrease of the peak height. Changing $\beta$ by 50% leads to only a 1% decrease in $g^{(2)}(0)$.

The sensitivity of the parameters to variation is easily understood by considering how the laser responds in different regions of its operating curve. Far below threshold, the modulated laser emits low-intensity light (fluorescence) linearly with the current. As we near threshold, the current occasionally fluctuates across the threshold, leading to bursts of light as the laser turns on. If we move closer to threshold, more fluctuations across threshold occur. This enhances the bunching until the growth of intensity fluctuation is balanced by the growing mean intensity. After this point, the bunching continuously decreases as the operating point is increased.

The $\beta$ parameter determines the slope and the shape of the laser threshold. If this is made smaller, the slope of the laser response increases. Below threshold, we expect a higher intensity for current fluctuations across threshold if the slope is steeper. Above threshold, the laser is operating with a large intensity proportional to the driving current. The slope does not affect the bunching since all fluctuations scale with the same linear response. The size of the bunching above threshold is insensitive to variations in $\beta$. Since we hold the threshold constant, changing $\beta$ effectively changes the decay rate of the laser cavity.

## 5.  CONCLUSIONS

We have a well-characterized source of correlated light from a noise-modulated diode laser. We have measured the intensity correlations using two experimental approaches: analysis of photocurrent time series and photon coincidence. The results show quantitative agreement with a simple model that considers only amplitude modulation of the laser. The linear version of the theory relates the Fourier transform of the spectral density of the noise to the intensity correlation with excellent quantitative agreement if the noise-current excursions are not too large. The behavior near threshold requires a model based on the steady state of laser rate equations that account for the nonlinearity of the threshold.

The variance of the intensity fluctuations is proportional to the noise power coupled to the laser. This permits a gradual modification of the statistics of the light. Below threshold, the value of $g^{(2)}(0)$ can greatly exceed the value of two for a chaotic source. We can control the size of bunching by varying the noise-current amplitude, and the time response by adjusting the spectrum of the noise current.

Such a modulated diode laser, with well-characterized intensity correlations, could be a very attractive source for experiments in cavity QED to explore the non-Markovian regime.

## REFERENCES

1.  F. T. Arrechi, E. Gatti, and A. Sona, Phys. Lett. **20**, 27 (1966).
2.  J. A. Abate, H. J. Kimble, and L. Mandel, Phys. Rev. A **14**, 788 (1976).
3.  K. Kaminishi, R. Roy, R. Short, and L. Mandel, Phys. Rev. A **24**, 370 (1981).
4.  P. Lett, R. Short, and L. Mandel, Phys. Rev. Lett. **52**, 341 (1984).
5.  P. Lett and E. C. Gage, Phys. Rev. A **39**, 1193 (1989).
6.  R. Graham, M. Höhnerbach, and A. Schenzle, Phys. Rev. Lett. **48**, 1396 (1982).
7.  R. Fox and R. Roy, Phys. Rev. A **35**, 1838 (1987).
8.  P. Jung, Th. Leiber, and H. Risken, Z. Phys. B **66**, 397 (1987); Th. Leiber, P. Jung, and H. Risken, Z. Phys. B **68**, 123 (1987).
9.  J. M. Noriega, L. Pesquera, M. A. Rodríguez, J. Casademunt, and A. Hernández-Machado, Phys. Rev. A **44**, 2094 (1991).
10.  J. J. Phillips, M. R. Young, and S. Singh, Phys. Rev. A **44**, 3239 (1991).
11.  R. G. W. Brown and R. S. Grant, Rev. Sci. Instrum. **58**, 928 (1987).
12.  M. Ohtsu and T. Tako, Prog. Opt. **25**, 191 (1988).
13.  B. R. Mollow, Phys. Rev. **175**, 1555 (1968).
14.  D. S. Elliot, M. W. Hamilton, K. Arnett, and S. J. Smith, Phys. Rev. Lett. **53**, 439 (1984).
15.  M. W. Hamilton, D. S. Elliot, K. Arnett, and S. J. Smith, Phys. Rev. A **33**, 778 (1986).
16.  K. Arnett, S. J. Smith, R. E. Ryan, T. Bergeman, H. Metcalf, M. W. Hamilton, and J. R. Brandenberger, Phys. Rev. A **41**, 2580 (1990).
17.  D. S. Elliot and S. J. Smith, J. Opt. Soc. Am. B **5**, 1927 (1988).
18.  R. Ryan, Ph.D. dissertation (State University of New York, Stony Brook, New York, 1993).
19.  J. Gea-Banacloche, Phys. Rev. Lett. **62**, 1603 (1989).
20.  J. Javanainen and P. L. Gould, Phys. Rev. A **41**, 5088 (1990).
21.  N. Ph. Georgiades, E. S. Polzik, K. Edamatsu, H. J. Kimble, and A. S. Parkins, Phys. Rev. Lett. **75**, 3426 (1995).

22. H. J. Carmichael, Phys. Rev. Lett. **70**, 2273 (1993).
23. C. W. Gardiner, Phys. Rev. Lett. **70**, 2269 (1993).
24. J. Gripp, S. L. Mielke, and L. A. Orozco, Phys. Rev. A **51**, 4974 (1995).
25. P. R. Rice and H. J. Carmichael, IEEE J. Quantum Electron. **QE-24**, 1351 (1988).
26. L. Mandel and E. Wolf, *Optical Coherence and Quantum Optics* (Cambridge U. Press, Cambridge, UK, 1995).
27. A. Siegman, *Lasers* (University Science Books, Mill Valley, Calif., 1986).
28. S. L. Mielke, G. T. Foster, and L. A. Orozco, Phys. Rev. Lett. **80**, 3948 (1998).
29. H. J. Carmichael, S. Singh, R. Vyas, and P. Rice, Phys. Rev. A **39**, 1200 (1989).
30. A. L. Lacaita, F. Zappa, S. Bigliardi, and M. Manfredi, IEEE Trans. Electron Devices **40**, 577 (1993).